BIOCHEMISTRY
including biophysical chemistry & molecular biology

Article

pubs.acs.org/biochemistry

Dimerization of Nitrophorin 4 at Low pH and Comparison to the K1A Mutant of Nitrophorin 1

Robert E. Berry,*,† Fei Yang, Tatiana K. Shokhireva, Angela M. Amoia, Sarah A. Garrett, Allena M. Goren, Stephanie R. Korte, Hongjun Zhang, Andrzej Weichsel, William R. Montfort,* and F. Ann Walker*

Department of Chemistry and Biochemistry, The University of Arizona, P.O. Box 210041, Tucson, Arizona 85721-0041, United States

Supporting Information

ABSTRACT: Nitrophorin 4, one of the four NO-carrying heme proteins from the salivary glands of *Rhodnius prolixus*, forms a homodimer at pH 5.0 with a K_d of ~8 μM. This dimer begins to dissociate at pH 5.5 and is completely dissociated to monomer at pH 7.3, even at 3.7 mM. The dimer is significantly stabilized by binding NO to the heme and at pH 7.3 would require dilution to well below 0.2 mM to completely dissociate the NP4-NO homodimer. The primary techniques used for investigating the homodimer and the monomer−dimer equilibrium were size-exclusion fast protein liquid chromatography at pH 5.0 and $^1H\{^{15}N\}$ heteronuclear single-quantum coherence spectroscopy as a function of pH and concentration. Preparation of site-directed mutants of NP4 (A1K, D30A, D30N, V36A/D129A/L130A, K38A, R39A, K125A, K125E, D132A, L133V, and K38Q/R39Q/K125Q) showed that the N-terminus, D30, D129, D132, at least one heme propionate, and, by association, likely also E32 and D35 are involved in the dimerization. The "closed loop" form of the A−B and G−H flexible loops of monomeric NP4, which predominates in crystal structures of the monomeric protein reported at pH 5.6 but not at pH 7.5 and which involves all of the residues listed above except D132, is required for dimer formation. Wild-type NP1 does not form a homodimer, but NP1(K1A) and native N-terminal NP1 form dimers in the presence of NO. The homodimer of NP1, however, is considerably less stable than that of NP4 in the absence of NO. This suggests that additional aspartate or glutamate residues present in the C-terminal region of NP4, but not NP1, are also involved in stabilizing the dimer.

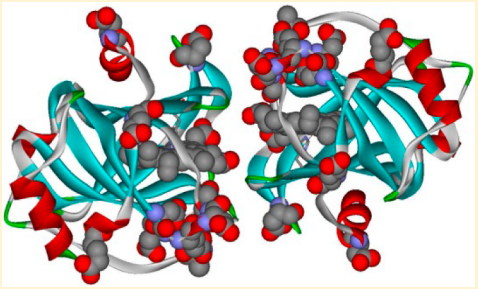

The nitrophorins (nitro = NO, phorin = carrier) make up a group of NO-carrying heme proteins found in the saliva of at least two species of blood-sucking insects, *Rhodnius prolixus*, the "kissing bug", which has four such proteins in the adult insect[1−5] and at least three additional nitrophorins in earlier stages of development,[6,7] and *Cimex lectularius*, the bedbug, which has only one.[8,9] These interesting heme proteins sequester NO that is produced by a nitric oxide synthase (NOS) that is similar to vertebrate constitutive NOS and is present in the endothelial cells of the salivary glands,[10−12] which keeps it stable for long periods of time by binding it as an axial ligand to a ferriheme center.[1,3−5] The nitrophorins are at a very high concentration in the salivary glands of *R. prolixus* (combined NP concentration estimated to be ~6−10 mM[a]), thus giving rise to the cherry red color[1] of the glands. To function in insect feeding, the nitrophorin proteins must efficiently pack in the gland and stably bind NO, despite its reactive nature. The ferriheme binding site is crucially important in stabilizing the bound NO for long periods of time in the salivary glands. Upon injection into the tissues of the victim, NO dissociates and diffuses through the tissues to the nearby capillaries to cause vasodilation and thereby allow more blood to be transported to the site of the wound. At the same time, histamine, whose role is to cause swelling, itching, and the beginning of the immune response, is released by mast cells and platelets of the victim in the region of the bite. In the case of the *Rhodnius* proteins, this histamine binds to the heme sites of the nitrophorins, hence preventing the insect's detection for a period of time.[13] These two properties of the nitrophorins of *R. prolixus* contribute to the transmission of the protozoan *Trypanasoma cruzi*, the vector of Chagas' disease,[14] to the victim, via the feces of the insect, which are left behind at the site of the bite[3] following the extended feeding time.

The *Rhodnius* nitrophorins of the adult insect, which have been named NP1−NP4 in reverse order of their abundance in the saliva,[2] occur as two pairs of similar sequence proteins, NP1 and NP4, which are 90% identical, and NP2 and NP3, which are 80% identical;[2] the overall level of sequence identity is only 38%. The sequences are shown in Figure S1 of the Supporting Information. These proteins have been investigated by a number of techniques (DOI: 10.1021/bi501305a),[1,3,15−40] and the solid state structures of one or more ligand complexes of NP1,[15,41] NP2,[42,43] and NP4[44−49] have been determined by X-ray crystallography. The structures are unique for heme proteins, in that the heme is located inside, but at the open end, of a β-barrel,[8,50] as shown in Figure 1, rather than in the

Received: October 17, 2014
Revised: December 8, 2014
Published: December 9, 2014

DOI: 10.1021/bi5013047
Biochemistry 2015, 54, 208−220

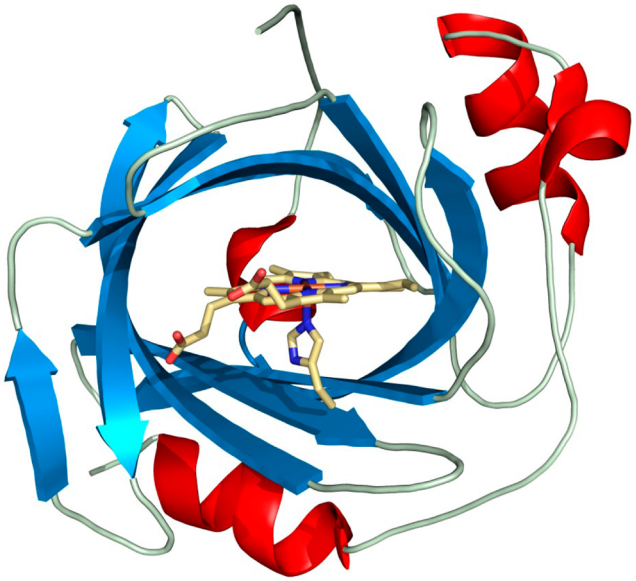

Figure 1. Structure of NP4. Shown are the protein backbone (blue for β-strands, red for α-helices, and gray for loops) and the heme (gold). Taken from Protein Data Bank entry 1X8O.

more commonly observed largely α-helical globin[51] or four-helix bundle[52] folds. The ferriheme molecule is bound to the protein via a histidine ligand, and the sixth coordination site is available to bind NO or other ligands. In the NO-off form *in vitro*, either water or ammonia, depending on buffer type, is bound to the sixth site.[41,44]

Although NP4 and quite a number of its axial ligand complexes have been crystallized and their structures determined to high resolution by single-crystal X-ray diffraction,[44−49] NP4 in solution at the low pH of the insect's saliva (5−6) is an equilibrium mixture of at least two forms, a monomer and a dimer; higher-order oligomers have also been claimed.[53] The previous report focused mainly on the gas-phase properties of NP4, which showed up to 14-mers present by mass spectrometry.[53] The work presented here focuses on the solution properties that are important to the reaction chemistry of NP4 and its NO complex in the salivary glands and the tissues of the victim. Our work has included the preparation and investigation of site-directed mutants to define which protein side chains are involved in dimerization. We find that NP4 is a dimer at pH 5.0 at ≥1 mM but a monomer at pH 7.3, the approximate pH of the victim's tissues; the dimer is much more stable when the ferriheme iron is bound to nitric oxide (NO).

Because the sequences of NP4 and NP1 are 90% identical, we were surprised that we had not observed a dimeric form for NP1 during our early studies of that protein.[15,17,19,21,23,25,28] However, NP1, like NP2 and NP3, has a charged amino acid at its N-terminus (Figure S1 of the Supporting Information), and during expression of any of these three genes, the methionine that results from translation of the start codon of the gene is not cleaved by the methionine aminopeptidase of *Escherichia coli*, thus leaving M0, with its relatively large side chain, at the N-terminus of these three proteins when they are isolated and purified. In the insect, the nitrophorins are expressed with an N-terminal signal sequence to target the protein for secretion into the salivary gland of the insect; cleavage of the signal sequence after secretion yields the mature N-terminus without methionine. The genes for the recombinant proteins, however, did not include the N-terminal signal sequence but rather began with the start codon, followed by the codon for the first amino acid of the protein. The M0 residue in the recombinant protein was not shown in the crystal structures of NP1 published before 2000,[15,41] because of the relatively low resolution of the structures (2.0−2.3 Å) and disorder at the N-terminus in the crystals, but mass spectrometry clearly shows the presence of M0 for recombinant NP1, as well as NP2[24] and NP3, as shown below. In contrast to NP1−NP3, NP4, with its N-terminal amino acid alanine, does not retain M0 when expressed recombinantly. We thus suspected that because NP1 [actually (M0)NP1] did not form a dimer, while NP4 did, the N-terminal region of the NP4 and NP1 proteins might be involved in the observed dimerization of NP4, and we have thus prepared the gene for the K1A mutant of NP1 as well as native N-terminal NP1 in this work.

Our precedent for this approach was our earlier work on the D1A mutant of NP2,[24] which we found had no M0 present when isolated and had properties markedly different from those of the (M0)NP2 obtained from simple expression of the recombinant gene.[24] Later, we also prepared native N-terminal NP2, with D1 as the first amino acid, by combining our NP2 gene with an export sequence provided by the pelB leader sequence from *Erwinia carotovora*, which is present in the pET-26b expression plasmid (Novagen), to export the protein to the periplasm.[29] When the export sequence was naturally cleaved in the *E. coli* periplasm, we were left with native N-terminal NP2, which could be purified in small quantities. The expression also had to be conducted in small batches, and thus, we have continued to use NP2(D1A) for experiments that require large quantities of protein. We found that these two proteins [NP2(D1A) and native N-terminal NP2] had essentially identical heme ^{1}H NMR spectra and ^{1}H{^{15}N} HSQC spectra and very similar reaction properties, except for the rate constant for NO binding at pH 7.5, which was a factor of 5 smaller, and the equilibrium K_d for NO, which was a factor of 5 larger for the native N-terminal NP2 than for NP2(D1A).[29] These findings suggest an important role for D1 in the reactivity of the protein,[29] which we have not as yet elucidated. We have likewise recently created N-terminal NP1 in the same manner but find again that NP1(K1A) is easier to prepare in large quantities.

We have found that the techniques of size-exclusion chromatography at pH 5.0 and multidimensional NMR spectroscopy over a range of pH values from 4.0 to 8.0 are the most useful for studying the dimer/monomer behavior of NP4 and its mutants, as well as NP1(K1A) and native N-terminal NP1 in solution, and we report our findings below.

EXPERIMENTAL PROCEDURES

Protein Sample Preparation. Cloning and expression plasmids have been reported previously.[35] Expression in *E. coli* was conducted as described previously,[35] which gives rise to inclusion bodies.

Denaturation. NP4 inclusion bodies (8 g) were cut into small pieces and added to 23 mg of dithiothreitol (DTT) and 17.2 g of guanidinium chloride; 100 mM sodium phosphate, pH 7.5 buffer was added to increase the total volume of the solution to 30 mL. Sixty microliters of the 500 mM EDTA solution was added, and the mixture was stirred until the inclusion bodies had dissolved. The denatured solution was then ultracentrifuged at 35K for 20 min to clarify it.

DOI: 10.1021/bi5013047
Biochemistry 2015, 54, 208−220

Renaturation. A renaturation buffer was prepared (70.1 g of NaCl, 3 mL of 500 mM EDTA, and 100 mM sodium phosphate, pH 7.5 buffer were added to a total volume of 1.5 L) and chilled to ~4 °C; 2.3 g of DTT was added to the stirred renaturation buffer before the clarified denatured solution was slowly dripped into the chilled renaturation buffer. The resulting renaturing solution was stirred overnight at 4 °C.

Apoprotein Purification. The renaturing solution was dialyzed three times into 100 mM sodium phosphate, pH 7.5 buffer at 4 °C, at 8 h intervals. Copious precipitate was observed. The precipitate was collected by centrifugation, and the solution was then concentrated in a stirred cell concentrator to a volume of ~20 mL. The solution was clarified by ultracentrifugation at 35K for 20 min. The crude aponitrophorin obtained after inclusion body refolding was concentrated and purified by size-exclusion chromatography, as shown in Figure S2a of the Supporting Information for NP4 (see Size-Exclusion Fast Protein Liquid Chromatography (FPLC) Purification and Analysis of NP4 for further details). Misfolded and aggregated protein molecules have larger hydrodynamic sizes and are eluted first. The final, correctly folded protein eluted last as the major peak. Fractions from this peak were collected. The 280 nm absorbance of the purified aponitrophorin fractions can be seen in Figure S2b of the Supporting Information for apo-NP4, eluting as a single peak at pH 5.0, with the retention volume expected for the ~20 kDa monomeric protein.

Holoprotein Formation and Purification. To obtain holonitrophorins, heme must be added. This was done by adding an excess of hemin [or the symmetrical hemin ("sym-hemin"), 2,4-dimethyldeuterohemin (Frontier Scientific, Logan, UT)] dissolved in a concentrated KOH solution to the purified aponitrophorin at pH 7.5, then adjusting the pH to 5.0 to precipitate the excess heme, and finally purifying the holonitrophorin by size-exclusion chromatography at pH 5.0 to remove any nonspecifically bound heme. In the cases of NP1−NP3, the nitrophorin eluted as a single peak with the retention volume expected for the ~20 kDa protein, but for NP4, two peaks were observed, as shown in Figure S2c of the Supporting Information. The retention volume for the second peak was close to what is expected for apo-NP4, but the first peak has a retention volume expected for a protein of approximately twice the size, a holo-NP4 homodimer. A UV−vis spectrum of the two peaks showed the expected 280 nm protein and 402 nm heme Soret maxima, as shown in Figure S3 of the Supporting Information. The first peak had a very good 280 nm to 402 nm absorbance ratio (R) of 3.4, consistent with high-spin, pure holo-NP4. The second peak had a very low R of 1.7, consistent with a mixture of apo- and holo-NP4 and perhaps other impurities. The second peak could be titrated with hemin a second time to yield an R of 3.2. The thus-purified apo- and holo-NP4 were stored in lyophilized form at −80 °C until they were used. The "sym-hemin" was used for reconstituting the NP4 protein whenever it was to be used for NMR investigations, to avoid the duplication of $^{1}H\{^{15}N\}$ HSQC cross-peaks from the two heme orientations, A and B, which are present in approximately equal concentrations at equilibrium when the unsymmetrical protohemin is used for reconstitution. ^{15}N-labeled samples of NP4 were prepared as reported recently for NP2(D1A).[31]

The following mutants of NP4 were prepared to see if they abolished dimerization: A1K, D30A, D30N, V36A/D129A/L130A, K38A, R39A, K125A, K125E, K38Q/R39Q/K125Q, D132A, and L133V; for contrast between (M0)NP1 and NP4, the K1A mutant of NP1 was prepared. These mutants were all created using standard site-directed mutagenesis techniques, and they were all purified as described for the wild-type protein.[25,31] Creation of the native N-terminal NP1 was conducted using the same procedures that were used previously for preparing native N-terminal NP2;[29] a C-terminal His_6 tag was included to aid in purification. Later it was found that using this His_6 tag could cause proteases of *E. coli* to copurify with the desired nitrophorin, and thus, the His_6 tag was deleted from the native N-terminal NP2 gene, as well as from the NP1 gene. Both forms were studied, as noted for native N-terminal NP2 in Table 3 below, but only the His_6-tagged form of native N-terminal NP1 was available when the size-exclusion chromatography was conducted (Figure 9 below).

Size-Exclusion Fast Protein Liquid Chromatography (FPLC) Purification and Analysis of NP4. A small analytical grade GE Healthcare Superdex75 size-exclusion column and a preparative-scale GE Healthcare HiPrep 26/60 Sephacryl 5−100 size-exclusion column with one or two 5 mL guard columns preceding it were used to separate NP4 into two major fractions at pH 5.0.[25] The buffer used at pH 5.0 was 20 mM sodium acetate containing 150 mM NaCl, while the buffer used at pH 7.5 for preliminary purification of apo-NP4 was 20 mM Tris-HCl containing 100 mM NaCl. There was no evidence that these concentrations of salt interfered with dimer formation. Molecular weight (MW) markers [myoglobin (17 kDa), NP2 (20 kDa), and ovalbumin (44 kDa)] were used to estimate the molecular weights of the two fractions, which appeared to be ~40 and ~20 kDa, respectively. At pH 5.0, the 40 kDa fraction, the dimer of NP4, provided an excellent means of purifying the protein from traces of hemin, apoprotein, and other impurities, and thus, NP4 purification in the Walker laboratory has routinely utilized size-exclusion FPLC at pH 5.0 to purify the NP4 protein since 2005. See Figures S2−S5 of the Supporting Information for a comparison of the pH 5.0 FPLC traces of the four nitrophorins of adult *R. prolixus*.

Kinetics of Release of NO from the Nitrophorins. Stopped-flow measurements of the rate of release of NO from the nitrophorins have been reported previously.[17,19,29] The instrument used in this study was the Olis Stopped-Flow RSM 100 instrument. All stopped-flow measurements showed decay curves that were monophasic.

NMR Data Collection. NMR spectra were collected over the temperature range of 25−30 °C, with the proton and carbon chemical shifts referenced to sodium 2,2-dimethyl-2-silapentane-5-sulfonate (DSS). $^{1}H\{^{15}N\}$ HSQC spectra were recorded on a Varian INOVA 600 spectrometer operating at a proton Larmor frequency of 599.70 MHz. The $^{1}H-^{15}N$ HSQC experiments were conducted using a 5 mm inverse cryogenic probe, with decoupling during acquisition. Attempts were also made to measure $H^{+}-D^{+}$ exchange rates using the experiment SOFAST HSQC,[54] but the rates for residues in the A−B and G−H loops were found to be too rapid to allow measurement of k_{ex} values.

Mass Spectrometry. Mass spectra were recorded on a Bruker Ultraflex III mass spectrometer using MALDI-TOF (matrix-assisted laser desorption ionization time-of-flight). Theoretical average molecular weights were calculated from the expected protein sequences using the Compute Mw tool on the ExPASy Server.[55]

X-ray Crystallography. Crystals for this study were grown by the hanging drop method, using a 1:1 mixture of protein (0.5 mM) and precipitant [2.2−3.5 M ammonium phosphate

DOI: 10.1021/bi5013047
Biochemistry 2015, 54, 208−220

(pH 7.5)] as previously described.[48] Some crystals were then soaked in pH 5.6 buffer in the presence of NO or other potential ligands.[56] Previous crystals were grown under two conditions, in 2.6 M ammonium phosphate (pH 7.5) and in 22% PEG 4000 (pH 5.6). Despite large changes in crystallization conditions, all crystals were isomorphous. Diffraction data were measured at the Advanced Photon Source (APS), Argonne National Laboratory, beamline 14-BMD, and at the Stanford Synchrotron Radiation Laboratory (SSRL), beamline 9-2. Structures were determined by molecular replacement using Protein Data Bank (PDB) entries 1X8O, 1X8P, and 1X8Q.[48] Model building and refinement were achieved with REFMACS[57] and the CCP4 package.[58] Model building was achieved with COOT.[59] Structural figures were prepared using PyMOL (DeLano Scientific, http://www.pymol.org/). Structural superpositioning was accomplished using the secondary structure alignment approach and the program SSM Superimpose.[60]

RESULTS AND DISCUSSION

Size-Exclusion FPLC Analysis of NP4 and Its Site-Directed Mutants. We examined NP4 dimerization by analytical size-exclusion FPLC, a rapid technique that allowed for efficiently examining many proteins and buffer conditions. While less quantitative than measurements using analytical ultracentrifugation or hydrogen−deuterium exchange, many more parameters could be readily examined using size-exclusion FPLC. As shown in Figure 2, size-exclusion FPLC shows that the NP4 dimer is stable at pH 5.0 and 1 mM but is significantly destabilized above pH 5.5, or at pH 5.0 at much lower concentrations. Serial dilution of the 1 mM sample at pH 5.0 shows that the single peak shifts from the approximate molecular weight of a pure dimer to that of a fairly pure monomer (molecular weight similar to that of NP2) by the time a concentration of 0.025 mM is reached. This concentration is too low for NMR studies, and thus, NMR investigations must be conducted at higher pH values and higher concentrations. For the reaction

$$M_2 \rightleftharpoons 2M, \text{ with } K_d = [M]^2/[M_2] \quad (1)$$

where M is the monomer and M_2 is the dimer, if we assume $[M] \sim [M_2]$ at a total NP4 concentration of 0.025 mM, then $K_d \sim 8.3$ μM. This is thus a rough estimate of the K_d of the high-spin, NO-off Fe(III) dimer form of NP4 at pH 5.0.

At pH 6.5, at a concentration of 0.8 mM, the dimer is not detectable, and the $^1H\{^{15}N\}$ HSQC spectrum looks almost identical to that obtained at pH 7.3, with very few cross-peaks moving between those two pH values (DOI: 10.1021/bi501305a), as we will see below. Those that do move can be followed, and thus, the pH 6.5 $^1H\{^{15}N\}$ HSQC map has been assigned from the pH 7.3 assignments, with intermediate spectra run to follow the cross-peak movements (DOI: 10.1021/bi501305a). Below pH 6.5, or by starting at pH 5.0 and increasing the pH, we see significant progressive changes that indicate a major concentration for both monomer and dimer. In an expanded section of the $^1H\{^{15}N\}$ HSQC map of 0.2 mM NP4 as the pH is increased from 5.0 (red) to 5.5 (green) to 6.0 (blue), we see in Figure 3 that some small peaks at pH 5.0 (labeled A) become much larger at pH 5.5 in a shifted position, and larger yet at pH 6.0, as would be expected for peaks of the monomer, thus telling us that at 0.2 mM, there is some monomer present at pH 5.0. As we increase the pH above 5.0, some amide NH peaks begin to disappear as a result of a decrease in the concentration of the dimer (labeled B); others do not exhibit a significant change in chemical shift with pH or a change in intensity (labeled C), indicating they are not directly involved in dimer formation (are not at the dimer interface). Finally, some peaks move only slightly but remain at approximately the same intensity (labeled D), indicating that they are involved in a small change in conformation or dynamics upon dimer formation. Thus, although a tedious process, following the movements of the individual peaks in the $^1H\{^{15}N\}$ HSQC spectrum of high-spin NP4 as the pH is decreased from 7.3 [where the assignment of all but approximately five amino acids of NP4 was conducted (DOI: 10.1021/bi501305a)] to 6.5 and below provides a means of determining which peaks are most affected by dimer formation and are thus likely to be at the dimer interface.

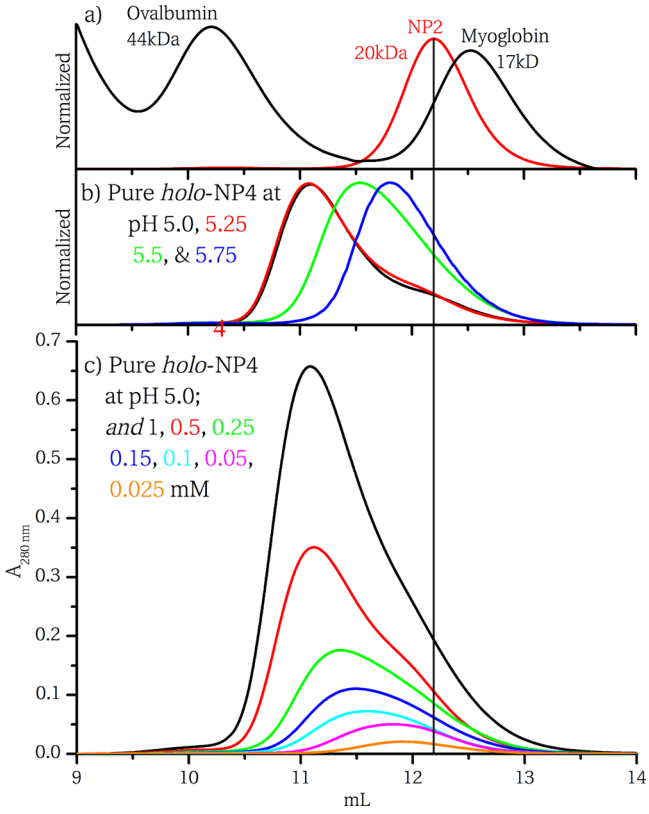

Figure 2. NP4 concentration and pH dependence, as measured by size-exclusion FPLC. Samples were run on an analytical grade Superdex75 size-exclusion column at 4 °C in 100 mM sodium acetate buffer with NaCl added to a total ionic strength of 220 mM: (a) NP2 and molecular weight standards at pH 5.0, (b) 1 mM NP4 injected into 50 μL and run at pH 5.0, 5.25, 5.5, and 5.75, and (c) NP4 injected into 50 μL, run at pH 5.0 and at various concentrations from 1 to 0.025 mM. The line connecting NP2 in panel a to the samples of panel c shows the expected retention volume of monomeric NP4, ~12.25 mL.

Attempts To Determine the Protein Side Chains That Promote Dimerization. Mutants of NP4 (A1K, D30A, D30N, V36A/D129A/L130A, K38A, R39A, K38Q/R39Q/K125Q, K125A, K125E, D132V, and L133V) were prepared, assuming that dimerization might involve an ion-paired structure using some of the many carboxyl groups at the open end of the protein, presumably interacting with lysine or arginine side chains on the surface of NP4 to create salt bridges.

DOI: 10.1021/bi5013047
Biochemistry 2015, 54, 208−220

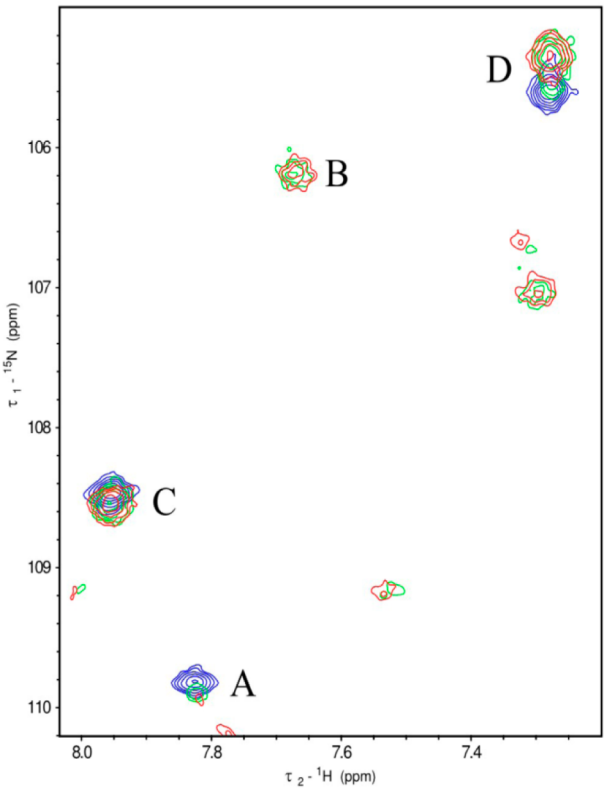

Figure 3. pH dependence of $^{15}N-^{1}H$ amide chemical shifts. An expanded section of the $^{1}H\{^{15}N\}$ HSQC spectrum of ^{15}N-labeled WT NP4 containing symmetrical hemin at 30 °C and ~0.2 mM, compared to pH 5.0, 5.5, and 6.0 (red, green, and blue, respectively). Peak A shows increasing intensity as the pH is increased. Peak B shows decreasing intensity. Peak C does not exhibit much change in chemical shift or intensity. Peak D shows a slight change in ^{15}N chemical shift.

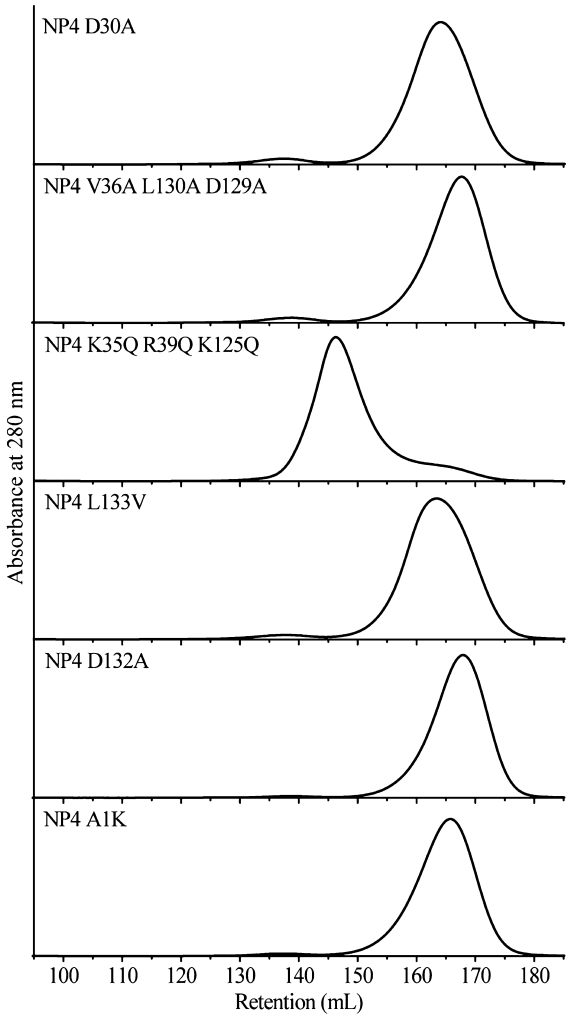

Figure 4. Size-exclusion fast protein liquid chromatography retention volumes of NP4 mutants. Plot of absorbance at 280 nm vs retention volume on a HiPrep 26/60 Sephacryl S-100 size-exclusion column connected in series with a 5 mL guard column, run with 100 mM sodium acetate, pH 5 buffer with 150 mM NaCl. The purified NP4 variant is indicated on each plot. Only the triple mutant, NP4(K38Q/R39Q/K125Q), runs as a dimer, showing that the charged side chains of this mutant are not involved in dimer formation but all of the others are. The A1K mutant has M0 present, which causes it to run as a monomer rather than as a dimer.

The D30A and D30N mutant proteins were early successes in this study. They both run through the size-exclusion column as monomers, as shown in Figure 4 (only D30A shown), thus indicating that D30 is involved in stabilizing the dimer. We cannot say whether other A–B loop carboxylates, E32, D34, or D35, are also involved, because we have not prepared site-directed mutants of those single amino acids, although as shown below, it is likely that at least some of them are involved. The V36A/D129A/L130A triple mutant also runs as a monomer, as will be discussed below.

Most interestingly, the A1K mutant of NP4 also runs as a monomer. This is particularly interesting, because by mutating A1 to K, we expected that M0 would not be cleaved by the methionine aminopeptidase of *E. coli*, as is the case for (M0)NP1. Indeed, the mass spectrum (MALDI-TOF) confirms that M0 is present, as listed in Table 1. Having lysine present as the first amino acid could confuse the issue, as far as the charge of the lysine side chain is concerned, but we are certain that rather than the charge of the lysine side chain, it is the size of M0, which we know from the crystal structure of (M0)NP2 as compared to NP2(D1A), that interferes with the closing of the A–B loop;[24] thus, (M0)NP2 is not a good model for how the native NP2 protein functions with respect to NO binding and release.[24] Thus, in terms of the size-exclusion chromatographic behavior of NP4 mutants, we believe that the size of M0 interferes with dimerization, and thus, the N-terminus of NP4 is somehow involved in dimer formation. This conclusion is further verified by the behavior of the K1A mutant of NP1 and native N-terminal NP1 (discussed below).

As for the lysine and arginine side chains that we thought might be involved in dimerization, the single mutants K38A, R39A, K125A, and K125E (not shown), as well as the triple mutant (K38Q/R39Q/K125Q), also run as dimers on the size-exclusion column at pH 5.0, as shown for the triple mutant in Figure 4. This fact, as well as the finding that the N-terminus is involved in dimer formation, strongly suggests that it is the low pH (5.0), where we know that most carboxylic acid side chains are protonated in the nitrophorins, that allows carboxyls to hydrogen-bond to other carboxyls, as they do in the low-pH (5.6) structures of monomeric NP4-NO (where the special environment of this part of the nitrophorins distorts the carboxyl pK_a values away from the typical value of ~4), to create the "closed loop" structure[45] that was used to develop a proposed mechanism for the release of NO from NP4 at the

DOI: 10.1021/bi5013047
Biochemistry 2015, 54, 208–220

Table 1. Mass Spectral Data for NP4, NP1, and NP2 and Some of Their Mutants

	observed MW (Da)	technique	calcd MW[a] (Da)	Δ[b]	ref
NP4 (from insect saliva) (N-terminus of ACTK...[c])	20914	LDMS	20267	647	2
NP4 (recombinant) (N-terminus of ACTK...)	20264	MALDI-TOF	20267	3	this work
NP4(A1K) (N-terminus of MKCTK...)	20455	MALDI-TOF	20455	0	this work
NP1 (from insect saliva) (N-terminus of KCTK...[c])	20378	LDMS	20483	105	2
NP1 (recombinant) (N-terminus of MKCTK...)	20608	MALDI-TOF	20614	6	this work
NP1(K1A) (N-terminus of ACTK...)	20425	MALDI-TOF	20426	1	this work
native N-terminal NP1 (N-terminus of KCTK...)	20475	MALDI-TOF	20483	8	this work
NP2 (from insect saliva) (N-terminus of DCST...[c])	19689	LDMS	19922	233	2
NP2 (recombinant) (N-terminus of MDCST...)	20053	MALDI-TOF	20053	0	24
NP2(D1A) (N-terminus of ACST...)	19878	MALDI-TOF	19878	0	24
native N-terminal NP2 (N-terminus of DCST...)	19917 − 23	MALDI-TOF	19922	<5	29

[a]Theoretical average molecular weight calculated from the expected protein sequence, using the Compute Mw tool on the ExPASy Server.[54] [b]Δ is the difference between the observed and calculated molecular weights. [c]N-Terminal amino acid sequence confirmed by amino-terminal sequencing.[2] Probably the LDMS (laser desorption mass spectrometry) scans were not properly calibrated for the molecular weights of the nitrophorin proteins.

pH (7.35) of the tissues of the victim.[47−49] This hydrogen-bonded structure is shown in Figure 5A, where the A−B and G−H loop residues are seen to be involved in an extensive hydrogen-bonded structure that involves both loops and the NH_3 group of D1, to close the loops and hold the NO, bound to Fe, in a hydrophobic pocket. Later work showed that the X-ray structures of both the D30A and D30N mutants have the NO-induced conformational change, as well as the pH dependence of NO release, largely abolished.[47]

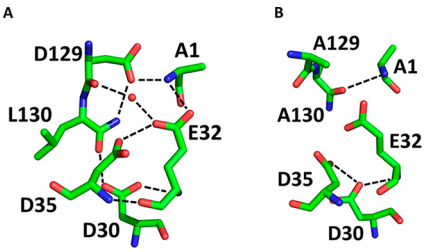

Figure 5. (A) Hydrogen-bonding interactions in the "closed loop" form of the monomeric NP4-NO complex at pH 5.6. The first version of this drawing was presented in ref 45. The hydrogen bond between D30 carboxyl and L130 carbonyl is a clear and important part of this structure. The hydrogen bond between D129 carboxyl and the amide NH group is that of G131. Because mutation of each of the individual residues D30 and D129 and the N-terminus prevents dimer formation, it is reasonable to assume that the "closed loop" conformation is necessary for dimer formation. (B) Minimal hydrogen bonding interactions in the "open loop" conformation of the triple mutant, NP4(V36A/D129A/D130A)-NO at pH 5.6, showing the much-reduced hydrogen-bonding network in the triple mutant, including the lack of hydrogen bonding between the G−H loop and the A−B loop. Thus, this triple mutant has an "open loop" structure.

As discussed below, D30 also appears to be a required part of the dimerization interface, as we will develop in the paragraphs to follow.

Returning to the comment that the V36A/D129A/L130A triple mutant runs through the size-exclusion column as a monomer, we see that D129 is intimately involved in the hydrogen-bonded "closed loop" structure of monomeric NP4-NO shown in Figure 5A. This structure suggests that it may well also be involved in the dimerization of NP4 at low pH. The structure of this mutant clearly shows that the hydrogen-bonded network of Figure 5A does not exist in this mutant, and instead, the A−B and G−H loops are in the fully open form at pH 5.6, as shown in Figures 5B and 6, where there is no hydrogen bonding between the A−B and G−H loops, and as they are in structures obtained at pH 7.5.[47−49] In fact, it is found that a number of the side chains involved in dimer formation are also those that were previously found to be involved in forming the "closed loop" structure of monomeric NP4-NO (Figure 5A). However, none of the lysine or arginine mutant proteins prepared in the hope of reducing the stability of the dimer by removing one potential ion-paired interaction or another led to the identification of any ion-paired interactions that might stabilize the dimer.

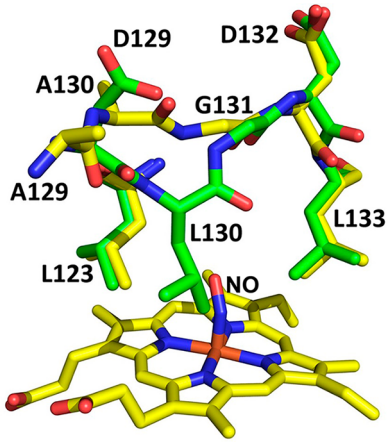

Figure 6. Superposition of two structures of NP4-NO complexes: wild-type NP4 (green bonds) (PDB entry 1ERX) and the NP4(V36A/D129A/D130A) triple mutant (yellow bonds; PDB entry 2OFR). Nitrogen atoms are colored blue and oxygens red, and the heme iron is colored dark red. The "closed loop" structure of the wild-type protein has residues L123 and L133 slightly shifted to the left in this view and shows the location of D129, sticking upward where it can hydrogen-bond to N-terminal A1, and L130 in the wild-type protein, with its side chain very close to the NO group.

All ligand complexes of holo-NP4 except for the histamine (Hm) complex also run as dimers at pH 5.0, as can be seen by the pH 5.0 size-exclusion column behavior of NP4-ImH and the NP4-NO complexes (Figure 7A). The Hm complex, however, is a monomer, and this is true at all pH values, including those below the first pK_a of Hm (6.0), where the concentration was increased to account for competition with the proton. The crystal structure of NP4-Hm at pH 7.5 (PDB

DOI: 10.1021/bi5013047
Biochemistry 2015, 54, 208−220

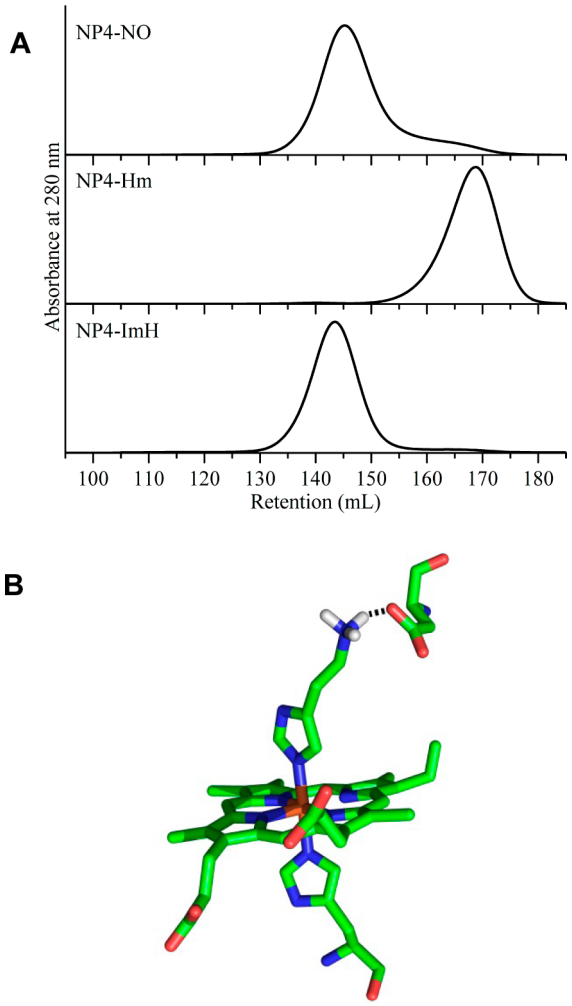

Figure 7. (A) Size-exclusion fast protein liquid chromatography retention volumes of NP4-ligand complexes. Plot of absorbance at 280 nm vs retention volume on a HiPrep 26/60 Sephacryl S-100 size-exclusion column connected in series with a 5 mL guard column, run with 100 mM sodium acetate, pH 5 buffer containing 150 mM NaCl. Purified NP4 (top) with nitric oxide bound and excess NO present in the running buffer to maintain the chemical equilibrium, (middle) with an excess of histamine bound to NP4 and 50 μM histamine present in the running buffer, and (bottom) with an excess of imidazole bound to NP4 and 50 μM imidazole present in the running buffer. The eluted protein was rosy red in each case, which is consistent with the ligand remaining bound during the elution. (B) Structure of the NP4-Hm complex, showing the hydrogen bond between the -NH_3^+ of histamine and the D30 carboxyl oxygen.

entry 1IKE) shows that the -NH_3^+ end of the histamine ligand is hydrogen-bonded to the carboxyl of D30,[46] while the imidazole part of the ligand, and indeed imidazole itself, is not involved in hydrogen bonding to the carboxyl of D30,[46] even through an intervening water molecule, as is the imidazole complex of NP2.[43] Similar structures of the hydrogen-bonded histamine complexes of NP1[41] and NP2[43] have also been reported, all of which show the same binding of the imidazole Nε atom of the histamine to the iron and the -NH_3^+ end hydrogen bonding to D30 carboxyl. Thus, by hydrogen bonding to D30, histamine prevents formation of the "closed loop" structure of monomeric NP4 that seems to be required for dimer formation. A water molecule is H-bonded to Nδ of histamine.

The NP4 apoprotein is also monomeric, as seen in Figure S2b of the Supporting Information (apo-NP4) as compared to Figure S2c of the Supporting Information (apo-NP4 + hemin). This may suggest that the heme carboxyls, which protrude from the front of the holoprotein, are also involved in dimerization; the crystal structure of apo-NP4 shows it to be well-folded and to have overall structural features almost identical to those of the holoprotein.[61]

At this point in our study, we had found that at least three of the residues involved in forming the closed loop structure seemed also to be involved in dimer formation, but we did not know for sure what stabilized the dimer at low pH. Then, serendipitously, we discovered that the L133V mutant of NP4 runs through the size-exclusion column at pH 5.0 as a monomer, although the peak is somewhat broader than other size-exclusion chromatographic peaks of the monomers of this study, as shown in Figure 4. Because at first glance the L133V mutant not being a dimer seemed to make no sense, the immediate neighbors in the protein sequence to Leu133 were examined; these neighbors are Asp132 and Tyr134, both of which, in the folded protein, are located on the outside of the β-barrel at the beginning of β-strand H, while Leu133 is inside the β-barrel, protruding into the heme distal pocket, directly above the heme, and with its terminal methyl groups in close van der Waals contact with the π electrons of one of the pyrrole rings of the heme. It was suggested that perhaps shortening the side chain of Leu133 might cause β-strand H of the β-barrel to move inward toward the heme. This, it was hypothesized, could pull Asp132 with it, perhaps burying it away from other surface side chains, and thus possibly preventing it from being involved with other protein side chains in dimerization. Although this reasoning turns out not to agree with structural features of the mutant, the D132A mutant of NP4 was prepared and was indeed found also to run as a monomeric protein on the size-exclusion column at pH 5.0, as shown in Figure 4. Thus, D132, along with the N-terminus, D30, and D129, is in some way involved in dimer formation.

Information from X-ray Crystallography. NP4 crystallizes as a monomer at both neutral pH (pH 7.4) and lower pH (pH 5.6), and with high salt or PEG as the precipitant. All conditions lead to crystals in the same space group (*C*2) with one molecule per asymmetric unit. These crystals diffract to extremely high resolution and allow for NO- and pH-dependent conformational changes in the A−B and G−H loops in the solid state. These results are consistent with our solution studies, which indicate NP4 is mainly monomeric at a concentration of 0.5 mM at pH 5.6 in the absence of NO (the NO complex was obtained by soaking existing crystals grown at pH 7.5 in an NO-containing solution). Thus, a direct view of the dimer contacts cannot be gained by crystallographic analyses.

Here, we show that dimer formation is hampered by high pH, modification of the N-terminus, mutation of Asp30 and Asp129, mutation of Asp132, binding of histamine to the heme iron, and probably mutation of other residues in the A−B and G−H loops, while dimer formation is aided by binding of NO to heme iron. All of the factors that hamper dimer formation alter the hydrogen-bonding arrangement that is key for forming the "closed loop" conformer (Figure 5A) of the monomeric protein, leading to the hypothesis that the closed conformation is required for dimer formation and may in fact lie at the dimer interface; NO binding stabilizes the "closed loop" conformation, with its hydrogen bonds (Figure 5A). Unexpectedly,

DOI: 10.1021/bi5013047
Biochemistry 2015, 54, 208−220

mutation of Leu133, which lies deep in the heme pocket, also disrupts dimer formation, but at first glance, it is unclear how this result fits with the closed conformer dimer interface hypothesis. To address how these mutations might alter dimer formation, we determined crystal structures of the NP4(L133V)-NH_3 complex (pH 7.5), the NP4(L133V)-NO complex (pH 5.6), and the NP4(V36A/D129A/L130A)-NO complex (pH 5.6), each to ~1.0 Å resolution (Table 2).

Table 2. Crystallographic Data for NP4(L133V)-NO, NP4(L133V)-NH_3, and NP4(V36A/D129A/L130A)-NO[56]

	NP4(L133V)-NO	NP4(L133V)-NH_3	NP4(V36A/D129A/L130A)-NO
PDB entry	2AT0	3C76	2OFR
pH	5.6	7.5	5.6
wavelength (Å)	0.98	0.90	0.90
resolution (Å)	1.00	1.07	1.00
total no. of reflections	341858	484613	882416
no. of unique reflections	83901	67479	79668
completeness (%)[a]	100/99	98/98	04.1/90.1
mean I/σ_I[a]	13.9/5.3	15.4/5.0	37.0/5.33
R_{sym}[a,b]	0.08/0.18	0.6/0.3	0.10/0.39
R_{cryst}/R_{free}[a,c]	0.14/0.16	0.14/0.17	0.22/0.25
rmsd[d]			
distances (Å)	0.01 (0.02)	0.02 (0.02)	0.01 (0.02)
angles (deg)	1.50 (2.00)	1.74 (2.00)	1.41 (2.00)

[a]Overall/outermost shell. [b]$R_{sym} = (\sum_h|I_h - \langle I\rangle|)/(\sum_h I_h)$, where $\langle I\rangle$ is the mean intensity of all symmetry-related reflections I_h. [c]$R_{cryst} = (\sum|F_{obs} - F_{calc}|)/\sum F_{obs}$. R_{free} as for R_{cryst}, using a random subset of the data (5%) not included in the refinement. [d]Root-mean-square deviation. Target values are in parentheses.

In the open conformation, the G−H loop (residues 125−132) is stabilized such that Leu130 is shifted away from the heme pocket, leading to greater heme pocket access.[45] A specific hydrogen-bonding network stabilizes this arrangement. In contrast, the A−B loop (residues 31−37) is disordered in the open conformation and does not adopt a single conformation. The "closed loop" conformation for the A−B loop can be detected in crystals of NP4 under "open conformation" conditions (high pH), because of the high resolution of NP4 structures, but has very poor electron density.[48] In the NP4(V36A/D129A/L130A)-NO structure (pH 5.6), which has mutations to both the A−B loop (Val36) and the G−H loop (Asp129 and Leu130), the G−H loop is open and density for the A−B loop is nearly nonexistent, as expected. This is consistent with the "closed loop" conformation being required for dimer formation, because this mutant protein does not dimerize. The NP4(L133V)-NH_3 structure (pH 7.5) displays an open conformation, as expected, and is very similar to that of the wild-type protein except for a small change in heme conformation where residue 133 contacts the heme (Leu123 and Leu133 contact the heme in the wild-type protein, leading to heme ruffling[46]). In the NP4(L133V)-NO structure (pH 5.6), the G−H loop is more disordered than in the wild-type structure and the closed conformation is less well-defined in the electron density map. The reason for this loss of the closed conformation is not entirely clear but may be related to the new position for Val133, which rotates toward Leu130 where it sterically interferes with the "fully closed" position for the Leu130 residue (in contact with NO). [Although Figure 6 is not of the NP4(L133V) mutant, it does show the close contact between L130 and the NO.] Nonetheless, the mutation hinders the "closed loop" conformation, which is the likely cause for the loss of dimer formation.

Asp132 is tightly constrained in all structures of the wild-type protein as well as the three mutants reported herein. The carboxyl oxygens of D132 hydrogen-bond to the backbone amides of residues 3 and 4, to the side chain OH group of Thr 3, to His120 Nε, and to an always-present water molecule (W288) that also hydrogen-bonds to the N-terminus. Thus, the D132A mutant would lose the function of stabilizing the N-terminus, thus perhaps disturbing the "closed loop" form of the protein. Certainly, as we see from the size-exclusion FPLC data at pH 5.0 shown in Figure 4, the fact that the D132A mutant, along with the N-terminal mutants D30A and D30N, and the triple mutant involving D129 all run as monomers strongly suggests that they are all involved in dimer formation and are reasonably close together but may not all be at the dimer interface.

Effect of Binding NO to NP4. As we have already shown in Figure 7, NP4-NO runs through the size-exclusion column as a dimer at pH 5.0. To investigate the NMR spectrum of NP4-NO, the $^1H\{^{15}N\}$ HSQC spectrum of a 3.7 mM ^{13}C- and ^{15}N-labeled sample of NP4 in the absence of NO at pH 7.3 was recorded and is shown in Figure 8 (left); this is the same doubly labeled sample that was used to assign the HSQC plot for the dynamics study (DOI: 10.1021/bi501305a). Then an excess of NO was added, and the $^1H\{^{15}N\}$ HSQC spectrum was again recorded. The $^1H\{^{15}N\}$ HSQC spectrum was ugly, with blotches of broad peaks suggesting the presence of monomer, dimer, and chemical exchange between them, as shown in Figure 8 (right). The 3.7 mM sample was diluted to 0.88 mM (a somewhat more than 4-fold dilution), with the intent of stabilizing the monomer. These two HSQC plots, at 3.7 and 0.88 mM, both with NO bound, can be seen side by side in Figure S6 of the Supporting Information. The dilution does not significantly change the $^1H\{^{15}N\}$ HSQC spectrum, other than the reduction in the signal-to-noise ratio expected due to dilution, although some of the smaller peaks seem to be a little more intense than the broad peaks in the 0.88 mM sample. Clearly, at 0.88 mM, the NP4-NO sample is still highly dimerized and is involved in chemical exchange between monomer and dimer. This was not observed for NP2 when NO was added, at pH 5.0 or 7.3,[31] or for either 3.7 or 0.88 mM high-spin NP4 in the absence of NO. The observed spectrum for NP4-NO (Figure 8, right) is consistent with a mixture of NP4-NO monomer and dimer and/or NP4-NO dimer in intermediate rate exchange with monomer. Attempts to assign this spectrum were prevented by chemical exchange. Thus, the NO complex of NP4 as a dimer is much more stable than high-spin NP4 itself, and it would require a much higher pH value and/or a much lower concentration of NP4-NO to produce an HSQC spectrum that contains cross-peaks from only monomeric protein. The question of why the NP4-NO dimer is more stable than the high-spin NP4 dimer is easily answered by the fact that NO binding helps to stabilize the "closed loop" structure of the monomer, which, in turn, should stabilize the NP4 dimer structure if the dimer structure depends upon the presence of the "closed loop" structure of the monomer.

DOI: 10.1021/bi5013047
Biochemistry 2015, 54, 208−220

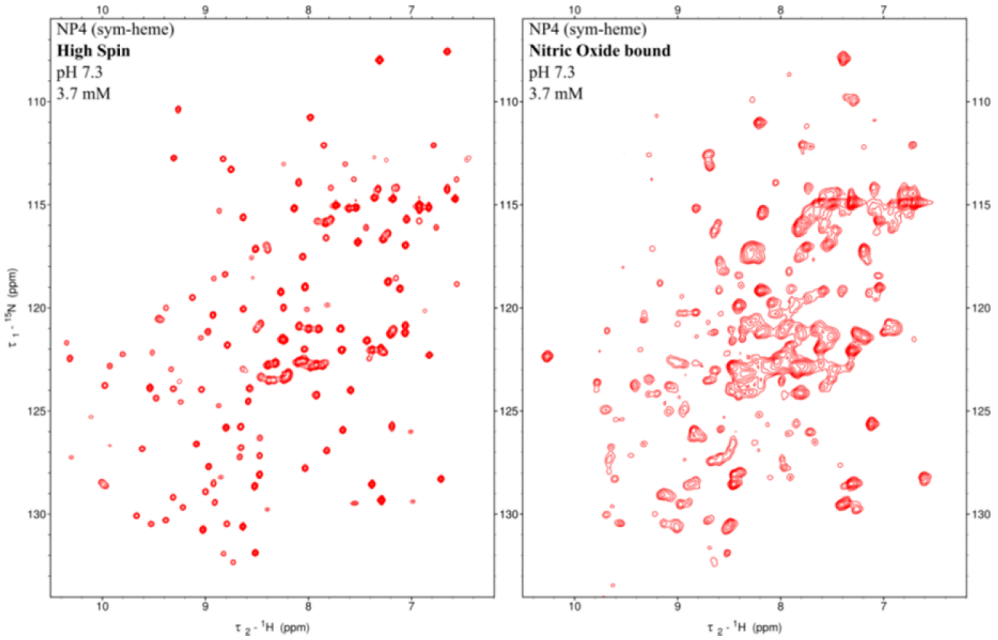

Figure 8. Two-dimensional amide $^{1}H-^{15}N$ chemical shift plot for NP4 in the absence and presence of nitric oxide. $^{1}H\{^{15}N\}$ HSQC spectrum of sym-hemin-containing NP4 at pH 7.3 and 3.7 mM in the absence of NO (left) and NP4(sym)-NO at pH 7.3 and 3.7 mM bound to NO (right). There is one unique $^{1}H-^{15}N$ cross-peak for each residue in the protein, and the assignment process permits the sequential assignment of essentially all of the amides of the protein. Although assignments of each cross-peak are not shown in this figure, the spectrum on the left has been fully assigned (except for four that could not be assigned, as well as three prolines that have no N–H).[29] The complete assignments are shown in Figure S2 of the Supporting Information.[29] We have not attempted to assign the spectrum on the right, because of the extensive chemical exchange between monomer and dimer that is evident.

Reducing the pH to 5.0 had a different and more significant effect, as can be seen in Figure S7 of the Supporting Information. At pH 5.0, the dimer should be very stable, and very little or no monomer should be present; thus, all the peaks observed in the $^{1}H\{^{15}N\}$ HSQC spectrum should be those of the dimer. None of the peaks yield blotches in the HSQC spectrum as we see in the right panel of Figure 8, and the majority of the peaks are well-formed and of similar size. Some of the peaks are of relatively low intensity, possibly because of dynamic processes or exchange with some monomer that might still be present. It may be possible to assign this spectrum, though it would be a difficult and lengthy task.

Comparison of NP4 to NP1. Because NP1 comprises 49%, as compared to 10% for NP4, of the nitrophorin protein in the insect saliva and because the protein sequences of the two are 90% identical (Figure S1 of the Supporting Information), we would have expected NP1 also to be a dimer at low pH. As mentioned in the introductory section and also shown in Figure S4 of the Supporting Information, recombinant NP1 is not a dimer at pH 5.0, and unpublished work confirms that it is not a dimer at any pH. However, we reasoned that this could be because M0, which is known to be present in the recombinant NP1 protein, blocks dimer formation. To test this hypothesis, we prepared the K1A mutant of NP1. We expected this protein to be a dimer, if the N-terminus of the protein is important to dimer formation, as our mutations of NP4, discussed above, had suggested. This is because we expected that this protein would have M0 cleaved in the process of protein expression, by the methionine aminopeptidase of *E. coli*, as is the case for NP4. Indeed, the mass spectrum of NP1(K1A) shows that Met0 is not present (Table 1). When the pH of the protein solution is lowered to 5.0 and the protein is run on the size-exclusion column, NP1(K1A) runs as a broad peak that encompasses the retention times expected for a dimer and a monomer, as shown in Figure 9, but when NO is added, NP1(K1A) runs as two peaks, the first of which is the dimer and the second of which is a mixture of apoprotein, impurities, and small amounts of monomer, as shown in Figure 9. The second peak might have been as large as it was because NO was being lost as the sample passed through the column, or because not enough excess hemin had been added to produce complete holoprotein. It is clear that the dimer is not as stable for NP1(K1A) as it is for NP4. The same is true for native N-terminal NP1; the presence of the C-terminal His_6 tag on this sample does not cause behavior different from that of NP1(K1A). Thus, NP1 without M0 is a dimer at pH 5.0 when bound to NO. This dimer has a K_d significantly larger than that of NP4 in the absence of NO but is stabilized by binding NO.

The fact that NP1(K1A) at pH 5.0 does not form a dimer as stable as that of NP4 suggests that there may be other protein side chains involved in the dimerization of NP4, not present in NP1, that we have not probed. Looking at Figure S1 of the Supporting Information, we find that except for the N-termini and residue 5 (a conservative replacement of L for I), there are no differences in the sequences of NP4 and NP1 until residue 76, where V of NP4 is E of NP1. Differences thereafter do not seem to be significant (L vs P, but possibly D90 of NP4 vs E90 of NP1 may be important because of side chain length), until nearly the end of the E–F loop, where A98 of NP4 is D98 of NP1. Thereafter, the differences are E159 for NP4 versus K159 for NP1, K162 for NP4 versus D162 for NP1, D168 for NP4 versus E168 for NP1, N170 for NP4 versus K170 for NP1, A172 for NP4 versus E172 for NP1, and D176 for NP4 versus V176 for NP1. Because NP4 forms the stronger dimer, and because all of the other residues found thus far to be involved in dimerization are carboxyls, except for the A1 amino group, we

DOI: 10.1021/bi5013047
Biochemistry 2015, 54, 208–220

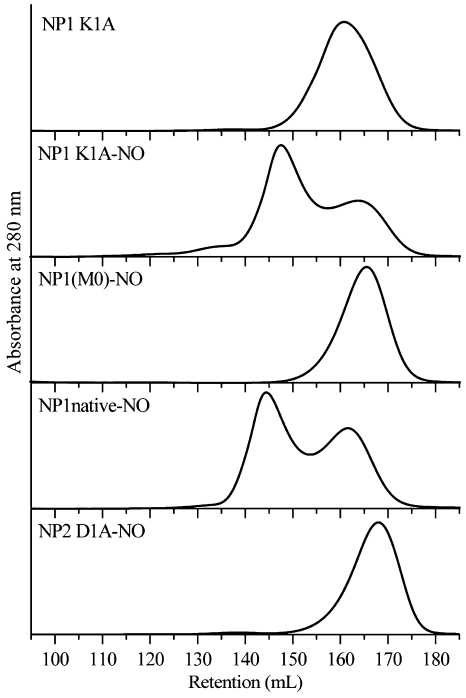

Figure 9. Size-exclusion fast protein liquid chromatography retention volumes of NP1 with various N-termini, each bound to nitric oxide. Plot of absorbance at 280 nm vs retention volume on a HiPrep 26/60 Sephacryl S-100 size-exclusion column connected in series with a 5 mL guard column, run with 100 mM sodium acetate, pH 5 buffer with 150 mM NaCl: NP1 K1A, NP1(K1A) with no ligand bound (H_2O-coordinated); NP1 K1A-NO, NP1(K1A) with nitric oxide bound, first time through the column; NP1(M0)-NO, NP1 expressed with a non-native M0 at the N-terminus resulting from the start codon and not cleaved, with nitric oxide bound; NP1native-NO, NP1 expressed with a leader sequence leading, at isolation, to native N-terminal NP1, with nitric oxide bound (note this sample has a C-terminal His_6 tag), first time through the column; NP2 D1A-NO, NP2(D1A) with nitric oxide bound.

conclude that having carboxyls available for NP4 would encourage dimer formation at pH 5.0. That could mean that D90, E159, D168, D176, and a heme propionate could potentially be involved. The two besides the heme propionate that are nearest the front face of the protein are D90 and D168 (Figure 10). There are also a number of aspartates and glutamates that are conserved between the two proteins that we have not probed, including E55 and D70, which are on the inside of the β-barrel, and a number of aspartates that are very far from the A−B and G−H loop region at the "front" of the protein. A nice grouping of residues that might contribute to dimer formation could be D132, E32 (it is on the surface of the H-bonded structure shown in Figure 5A and may be able to participate in H-bonding for both the monomer and the dimer), D34 (which sticks out from the "closed loop" group and is not involved in the "closed loop" form of Figure 5A), D90, and a heme carboxylate. E168, D176, and E159 might be involved, as well, as may be some of the conserved aspartates colored red in Figure S1 of the Supporting Information, which contribute for both NP1 and NP4, but beyond pointing these out, we cannot suggest a set of actual side chain interactions that stabilize the dimer of NP4 at pH 5.0 to an extent much greater than that of NP1.

Kinetics of Dissociation of NO from NP4, NP1, and NP2. A study of the binding of NO to and dissociation of NO

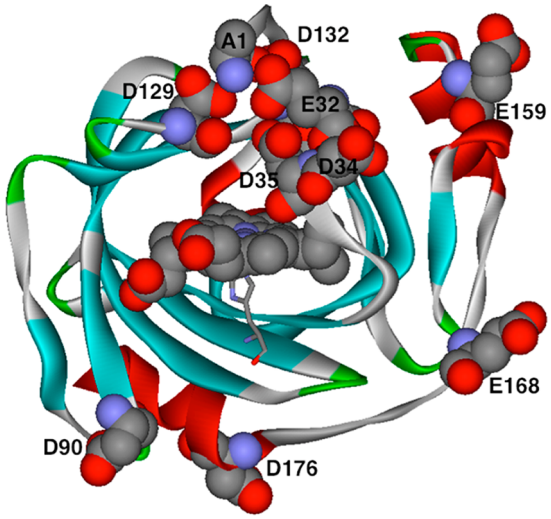

Figure 10. Structure of NP4 drawn to emphasize the carboxyl groups that are known to be or may be involved in dimerization. Carboxyls of the A−B (D30, E32, and D35) and G−H (D129) loops and the A1 amino group, known to be involved in stabilizing the "closed loop" form of the nitrophorins shown in Figure 5A, plus those shown to be involved in dimerization [D132, possibly D34, a heme carboxyl, and some, but probably not all, of the carboxyls on the front outer edge of the protein (D90, E159, E168, and D176, with the most probable underlined)]. PDB entry 1ERX.

from the four nitrophorins of *R. prolixus* was reported in 2000,[17] but in two of the three proteins for which we have crystallographic data, those measurements were taken before the X1A (X = K for NP1 and D for NP2 and NP3) or native N-terminal proteins were prepared and studied, meaning that the presence of M0 certainly affected the K_d values obtained and could have led to the presence of some dimer of NP1 and NP4 at pH 5.0 if the concentrations of the solutions were sufficiently high (however, they were generally 10 μM,[17] which was used in the recent studies). Dissociation of NO from the dimers should be multiphasic and slower than from the monomers. Therefore, we have recently measured the K_d values for NO release at pH 5.0 and 7.5 in dilute solution (5−10 μM in 100 mM sodium phosphate buffer). The results are listed in Table 3, where it can be seen that indeed, having M0 present increased the K_d for the loss of NO from NP1 by a factor of 20 and from NP2 by a factor 1.6 at pH 5.0, and by a factor of 2 for NP1 and a factor of 1.7 for NP2 at pH 7.5. The K_d for the loss of NO from NP4 is 0.6 times that from NP1 at pH 5.0 but 1.4 times that of NP1 at pH 7.5, which could suggest that NP4 is partially dimerized at pH 7.5. We know that the NP4 dimer is much more stable at pH 5.0 than at pH 7.3, it is much more stable when bound to NO than in its absence, and it is much more stable than the NP1 dimer under all conditions. Thus, dimerization may have contributed to the multiphasic kinetics observed in the earlier kinetics study,[17] except that bi- or multiphasic kinetics were observed for all four nitrophorins,[17] while it is clear from this work that (M0)NP1 and (M0)NP2 do not form dimers under any conditions; it is also unlikely that (M0)NP3 forms a dimer under any conditions because the similarity of its sequence to that of NP2, as well as the presence of M0.

Physiological Functions of the NP1 and NP4 Dimers. Our current understanding of the dimers of NP1 and NP4 is that their existence requires the presence of the "closed loop" forms of the proteins (Figure 5A), and they are stabilized by the

DOI: 10.1021/bi5013047
Biochemistry 2015, 54, 208−220

Table 3. Kinetic Data (K_d values for NO dissociation) for Various Constructs of Nitrophorins 1, 2, and 4

nitrophorin	extra-native	NO K_d (s^{-1}) pH 5.0	NO K_d (s^{-1}) pH 7.5	ref
(M0)NP1	M-KC...	0.20 ± 0.01	2.2 ± 0.01[a]	17
(M0)NP1	M-KC...	0.426 ± 0.005	2.32 ± 0.07	this work
(M0)NP1sym[b]	M-KC...	0.218 ± 0.004	2.66 ± 0.27	this work
Nat. N-term NP1[c]	KC...	0.032 ± 0.011	1.11 ± 0.04	this work
NP4	AC...	0.14 ± 0.01	2.6 ± 0.1[a]	17
NP4	AC...	0.020 ± 0.003	1.60 ± 0.11	this work
(M0)NP2	M-DC...	0.05 ± 0.01	0.12 ± 0.01[a]	17
(M0)NP2	M-DC...	0.049 ± 0.002	0.161 ± 0.005	29
NP2(D1A)	AC...	0.015 ± 0.005	0.089 ± 0.002	29
Nat. N-term NP2[c]	DC...	0.030 ± 0.002	0.093 ± 0.002	29
Nat. N-term NP2[d]	DC...	0.031 ± 0.002	0.099 ± 0.002	this work

[a]Measured at pH 8.0 rather than pH 7.5. [b](M0)NP2sym is (M0)NP2 containing the symmetrical heme, 2,4-dimethyldeuterohemin. [c]No C-terminal His_6 tag present. [d]C-Terminal His_6 tag present.

binding of NO to the ferriheme. When the residues of the A−B and G−H loops are hydrogen-bonded as they are in Figure 5A, to create the "closed loop" structure, the other carboxyls found to be involved (D132, possibly E32 and D34, at least one heme propionate, and probably some from the C-terminal loops and helices) can form the dimeric structures at pH 5.0, which begin to weaken even at pH 5.5.

NP1 and NP4 make up nearly 60% of the nitrophorin content of the saliva of adult *R. prolixus*. Dimer formation may provide additional stabilization of the NO complex in the insect salivary gland, where storage is required, by protecting the NO moiety from escape or reaction with other molecules. Dimerization may also allow for more efficient packing of the nitrophorin protein in the salivary gland, where the NP-NO concentration is quite high (as high as 6−10 mM[b]). However, with these two proteins being present in the salivary glands as dimers, which must dissociate into monomers before NO can leave each monomer (assuming that the dimer does involve the "closed loop" form of the protein), it is likely that the kinetics of NO release in the tissues are actually more complex than what can be simulated and measured *in vitro*.

■ ASSOCIATED CONTENT

Supporting Information

Nitrophorin sequences, additional size-exclusion FPLC traces, and $^1H\{^{15}N\}$ HSQC spectra of the NP4-NO dimer at two concentrations at pH 7.3 and one concentration at pH 5.0. This material is available free of charge via the Internet at http://pubs.acs.org.

Accession Codes

Coordinates for all structures reported have been deposited in the Protein Data Bank (PDB entries 3C76, 2AT0, and 2OFR).

■ AUTHOR INFORMATION

Corresponding Authors

*E-mail: rberry@umassd.edu. Telephone: (520) 399-8804.

*E-mail: montfort@email.arizona.edu. Telephone: (520) 621-1884.

*E-mail: awalker@email.arizona.edu. Telephone: (520) 621-8645.

Present Address

[†]R.E.B.: Department of Chemistry & Biochemistry, University of Massachusetts—Dartmouth, SENG-311A, 285 Old Westport Rd., North Dartmouth, MA 02747.

Funding

This work was supported by National Institutes of Health Grants HL054826 (F.A.W.), HL062969 (W.R.M.), and T32 GM008659 (A.M.A.) and the ARCS Foundation (A.M.A.). Portions of this research were conducted at the Stanford Synchrotron Radiation Laboratory, a national user facility operated by Stanford University on behalf of the U.S. Department of Energy. Diffraction data were also measured at BioCARS Sector 14, Advanced Photon Source, Argonne National Laboratory, which was supported by the U.S. Department of Energy under Contract W-31-109-Eng-38. Use of BioCARS Sector 14 was supported by the National Institutes of Health, National Center for Research Resources, via Grant RR07707.

Notes

The authors declare no competing financial interest.

■ ACKNOWLEDGMENTS

Undergraduates and high school students who prepared or characterized site-directed mutants of NP4 for this project include Martin Guerbadot, Maxim N. Shokhirev, William J. Golden, Arthur Y. W. Ho, Briana Broussard, Elizabeth J. Kennedy, David A. Terry, Anna E. Stahler Lueck, and Cari D. Natvig. We are grateful to these young scientists for their contributions to this work.

■ ADDITIONAL NOTES

[a]J. M. C. Ribeiro, personal communication.
[b]J. M. C. Ribeiro, personal communication.

■ REFERENCES

(1) Ribeiro, J. M. C., Hazzard, J. M. H., Nussenzveig, R., Champagne, D., and Walker, F. A. (1993) Reversible Binding of Nitric Oxide by a Salivary Nitrosylheme Protein from the Blood-Sucking Insect, *Rhodnius prolixus*. *Science 260*, 539−541.

(2) Champagne, D. E., Nussenzveig, R. H., and Ribeiro, J. M. C. (1995) Purification, Partial Characterization, and Cloning of Nitric Oxide-carrying Heme Proteins (Nitrophorins) from Salivary Glands of the Blood-Sucking Insect *Rhodnius prolixus*. *J. Biol. Chem. 270*, 8691−8695.

(3) Walker, F. A., Ribeiro, J. M. C., and Montfort, W. R. (1999) Novel NO-Liberating Heme Proteins from the Saliva of Blood-Sucking Insects. In *Metal Ions in Biological Systems, Vol. 36, Interrelations between Free Radicals and Metal Ions in Life Processes* (Sigel, H., and Sigel, A., Eds.) pp 619−661, Marcel Dekker, New York.

(4) Walker, F. A., and Montfort, W. R. (2001) The Nitric Oxide-Releasing Heme Proteins from the Saliva of the Blood-Sucking Insect *Rhodnius prolixus*. In *Advances in Inorganic Chemistry* (Mauk, G., and Sykes, A. G., Eds.) Vol. *51*, Chapter 5, pp 295−358, Academic Press, San Diego.

(5) Walker, F. A. (2005) Nitric Oxide Interaction with Insect Nitrophorins, and Thoughts on the Electron Configuration of the $\{FeNO\}^6$ Complex. *J. Inorg. Biochem. 99*, 216−236.

(6) Moreira, M. F., Coelho, H. S., Zingali, R. B., Oliveira, P. L., and Masuda, H. (2003) Changes in Salivary Nitrophorin Profile During

DOI: 10.1021/bi5013047
Biochemistry 2015, 54, 208−220

the Life Cycle of the Blood-Sucking Bug *Rhodnius prolixus*. *Insect Biochem. Mol. Biol. 33*, 23−28.
(7) Andersen, J. F., Gudderra, N., Francischetti, I. M. B., Valenzuela, J. G., and Ribeiro, J. M. C. (2004) Recognition of Anionic Phospholipid Membranes by an Antihemostatic Protein from a Blood-Feeding Insect. *Biochemistry 43*, 6987−6994.
(8) Valenzuela, J. G., Walker, F. A., and Ribeiro, J. M. C. (1995) A Salivary Nitrophorin (NO-Carrying Heme Protein) in the Bedbug, *Cimex lectularius*. *J. Exp. Biol. 198*, 1519−1526.
(9) Weichsel, A., Maes, E. M., Andersen, J. F., Valenzuela, J. G., Shokhireva, T. Kh., Walker, F. A., and Montfort, W. R. (2005) Heme-Assisted Nitrosothiolation of a Proximal Thiol in a Nitric Oxide Transport Protein. *Proc. Natl. Acad. Sci. U.S.A. 102*, 594−599.
(10) Ribeiro, J. M. C., and Nussenzveig, R. H. (1993) Nitric Oxide Synthase Activity from a Hematophagous Insect Salivary Gland. *FEBS Lett. 330*, 165−168.
(11) Nussenzveig, R. H., Bentley, D. L., and Ribeiro, J. M. C. (1995) Nitric-Oxide Loading of the Salivary Nitric-Oxide-Carrying Hemoprotein (Nitrophorin) in the Bloodsucking Bug *Rhodnius prolixus*. *J. Exp. Biol. 198*, 1093−1098.
(12) Yuda, M., Hirai, M., Miura, K., Matsumura, H., Ando, K., and Chinzei, Y. (1996) cDNA Cloning, Expression and Characterization of Nitric-Oxide Synthase from the Salivary Glands of the Blood-Sucking Insect *Rhodnius prolixus*. *Eur. J. Biochem. 242*, 807−812.
(13) Ribeiro, J. M. C., and Walker, F. A. (1994) High Affinity Histamine-Binding and Anti-Histaminic Activity of the Salivary NO-Carrying Heme Protein of *Rhodnius prolixus*. *J. Exp. Med. 180*, 2251−2257.
(14) Kirchhoff, L. V. (1993) American Trypanosomiasis (Chagas' Disease): A Tropical Disease Now in the United States. *N. Engl. J. Med. 329*, 639−644.
(15) Ding, X. D., Weichsel, A., Andersen, J. F., Shokhireva, T. Kh., Balfour, C., Pierik, A. J., Averill, B. A., Montfort, W. R., and Walker, F. A. (1999) Nitric Oxide Binding to the Ferri- and Ferroheme States of Nitrophorin 1, a Reversible NO-Binding Heme Protein from the Saliva of a Blood-Sucking Insect, *Rhodnius prolixus*. *J. Am. Chem. Soc. 121*, 128−138.
(16) Maes, E. M., Walker, F. A., Montfort, W. R., and Czernuszewicz, R. S. (2001) A Resonance Raman Spectroscopic Study of Nitrophorin 1, a Nitric Oxide-Binding Heme Protein from the Saliva of the Blood-Sucking Insect *Rhodnius prolixus*, and Its NO and Cyanide Adducts. *J. Am. Chem. Soc. 123*, 11664−11672.
(17) Andersen, J. F., Ding, X. D., Balfour, C., Champagne, D. E., Walker, F. A., and Montfort, W. R. (2000) Kinetics and Equilibria in Ligand Binding by Nitrophorins 1−4: Evidence for Stabilization of a NO-Ferriheme Complex through a Ligand-Induced Conformational Trap. *Biochemistry 39*, 10118−10131.
(18) Shokhireva, T. K., Berry, R. E., Uno, E., Balfour, C. A., Zhang, H., and Walker, F. A. (2003) Electrochemical and NMR Spectroscopic Studies of Distal Pocket Mutants of Nitrophorin 2: Stability, Structure and Dynamics of Axial Ligand Complexes. *Proc. Natl. Acad. Sci. U.S.A. 100*, 3778−3783.
(19) Berry, R. E., Ding, X. D., Shokhireva, T. K., Weichsel, A., Montfort, W. R., and Walker, F. A. (2004) Axial Ligand Complexes of the *Rhodnius* Nitrophorins: Electrochemistry, Binding Constants, and Structures of the 4-Iodopyrazole and Imidazole Complexes of NP4. *JBIC, J. Biol. Inorg. Chem. 9*, 135−144.
(20) Shokhireva, T. K., Shokhirev, N. V., and Walker, F. A. (2003) Assignment of Heme Resonances and Determination of the Electronic Structures of High- and Low-Spin Nitrophorin 2 by ^{1}H and ^{13}C NMR Spectroscopy: An Explanation of the Order of Heme Methyl Resonances in High-Spin Ferriheme Proteins. *Biochemistry 42*, 679−693.
(21) Shokhireva, T. K., Smith, K. M., Berry, R. E., Shokhirev, N. V., Balfour, C., Zhang, H., and Walker, F. A. (2007) Assignment of the Ferriheme Resonances for the High-Spin Form of Nitrophorins 1 and 4 by ^{1}H and ^{13}C NMR Spectroscopy: Comparison to Structural Data Obtained from X-ray Crystallography. *Inorg. Chem. 46*, 170−178.
(22) Shokhireva, T. K., Berry, R. E., Zhang, H., Shokhirev, N. V., and Walker, F. A. (2008) Assignment of Ferriheme Resonances for High- and Low-Spin Forms of Nitrophorin 3 by ^{1}H and ^{13}C NMR Spectroscopy and Comparison to Nitrophorin 2: Heme Pocket Structural Similarities and Differences. *Inorg. Chim. Acta 361*, 925−940.
(23) Shokhireva, T. K., Weichsel, A., Smith, K. M., Berry, R. E., Shokhirev, N. V., Balfour, C., Zhang, H., Montfort, W. R., and Walker, F. A. (2007) Assignment of the Ferriheme Resonances for Low-Spin Complexes of Nitrophorins 1 and 4 by ^{1}H and ^{13}C NMR Spectroscopy: Comparison to Structural Data Obtained from X-ray Crystallography. *Inorg. Chem. 46*, 2041−2056.
(24) Berry, R. E., Shokhireva, T. K., Filippov, I., Shokhirev, M. N., Zhang, H., and Walker, F. A. (2007) Effect of the N-Terminus on Heme Cavity Structure, Ligand Equilibrium and Rate Constants, and Reduction Potentials of Nitrophorin 2 from *Rhodnius prolixus*. *Biochemistry 46*, 6830−6843.
(25) Shokhireva, T. K., Shokhirev, N. V., Berry, R. E., Zhang, H., and Walker, F. A. (2008) Assignment of Ferriheme Resonances for High- and Low-Spin Forms of the Symmetrical Hemin-Reconstituted Nitrophorins 1−4 by ^{1}H and ^{13}C NMR Spectroscopy: The Dynamics of Heme Ruffling Deformations. *JBIC, J. Biol. Inorg. Chem. 13*, 941−959.
(26) Yang, F., Knipp, M., Berry, R. E., Shokhireva, T. K., Zhang, H., and Walker, F. A. (2009) ^{1}H and ^{13}C NMR Spectroscopic Studies of the Ferriheme Resonances of the Low-Spin Imidazole, Histamine and Cyanide Complexes of *wt* Nitrophorin 2 and NP2(V24E) as a Function of pH. *JBIC, J. Biol. Inorg. Chem. 14*, 1077−1095.
(27) Shokhireva, T. K., Berry, R. E., Zhang, H., Shokhirev, N. V., and Walker, F. A. (2011) NMR Studies of Nitrophorin Distal Pocket Side Chain Effects on the Heme Orientation and Seating of NP2 as Compared to NP1. *J. Inorg. Biochem. 105*, 1238−1257.
(28) Shokhireva, T. K., and Walker, F. A. (2012) Assignment of the ^{1}H NMR Resonances of Protein Residues in Close Proximity to the Heme of the Nitrophorins: Similarities and Differences among the Four Proteins from the Saliva of the Adult Blood-Sucking Insect, *Rhodinus prolixus*. *JBIC, J. Biol. Inorg. Chem. 17*, 911−926 1303.
(29) Berry, R. E., Muthu, D., Garrett, S. A., Shokhireva, T. K., Zhang, H., and Walker, F. A. (2012) Native N-Terminus Nitrophorin 2 from the Kissing Bug: Similarities to and Differences from NP2(D1A). *Chem. Biodiversity 9*, 1739−1755.
(30) Abriata, L. A., Zaballa, M.-E., Berry, R. E., Yang, F., Zhang, H., Walker, F. A., and Vila, A. J. (2013) Electron Spin Density on the Axial His Ligand of High-Spin and Low-Spin Nitrophorin 2 Probed by Heteronuclear NMR Spectroscopy. *Inorg. Chem. 52*, 1285−1295.
(31) Muthu, D., Berry, R. E., Zhang, H., and Walker, F. A. (2013) NMR Studies of the Dynamics of Nitrophorin 2 Bound to Nitric Oxide. *Biochemistry 52*, 7910−7925.
(32) Berry, R. E., Muthu, D., Shokhireva, T. K., Garrett, S. A., Goren, A. M., Zhang, H., and Walker, F. A. (2014) NMR Investigations of Nitrophorin 2 Belt Side Chain Effects on Heme Orientation and Seating of Native N-Terminus NP2 and NP2(D1A). *JBIC, J. Biol. Inorg. Chem. 19*, 577−593.
(33) Astashkin, A. V., Raitsimring, A. M., and Walker, F. A. (1999) Two- and Four-Pulse ESEEM Studies of the Heme Binding Center of a Low-Spin Ferriheme Protein: The Importance of a Multi-Frequency Approach. *Chem. Phys. Lett. 306*, 9−17.
(34) Wegner, P., Benda, R., Schünemann, V., Trautwein, A. X., Berry, R. E., Balfour, C. A., Wert, D., and Walker, F. A. (2002) How a Blood Sucking Insect Gets Its Meal: The Ferriheme Proteins Nitrophorin 2 and 4 Studied by Mössbauer Spectroscopy. *Hyperfine Interact. (C), Proc. Int. Conf. Appl. Moessbauer Eff. 5*, 253−256.
(35) Andersen, J. F., Champagne, D. E., Weichsel, A., Ribeiro, J. M. C., Balfour, C. A., Dress, V., and Montfort, W. R. (1997) Nitric Oxide Binding and Crystallization of Recombinant Nitrophorin 1, a Nitric Oxide Transport Protein from the Blood-Sucking Bug *Rhodnius prolixus*. *Biochemistry 36*, 4423−4428.
(36) Abbruzzetti, S., He, C., Ogata, H., Bruno, S., Viappiani, C., and Knipp, M. (2012) Heterogeneous Kinetics of the Carbon Monoxide

DOI: 10.1021/bi5013047
Biochemistry 2015, 54, 208−220

Association and Dissociation Reaction to Nitrophorin 4 and 7 Coincide with Structural Heterogeneity of the Gate-Loop. *J. Am. Chem. Soc. 134*, 9986−9998.
(37) Benabbas, A., Ye, X., Kubo, M., Zhang, Z., Maes, E. M., Montfort, W. R., and Champion, P. M. (2010) Ultrafast Dynamics of Diatomic Ligand Binding to Nitrophorin 4. *J. Am. Chem. Soc. 132*, 2811−2820.
(38) Moeser, B., Janoschka, A., Wolny, J., Filipov, I., Chumakov, A. I., Walker, F. A., and Schünemann, V. (2012) Nuclear Inelastic Scattering of Heme Proteins: From Iron-Ligand Vibrations to Low Energy Protein Modes. *Hyperfine Interact. 206*, 19−22.
(39) Moeser, B., Janoschka, A., Wolny, J. A., Paulsen, H., Filippov, I., Berry, R. E., Zhang, H., Chumakov, A. I., Walker, F. A., and Schünemann, V. (2012) Nuclear Inelastic Scattering and Mössbauer Spectroscopy as Local Probes for Ligand Binding Modes and Electronic Properties in Proteins: Vibrational Behavior of a Ferriheme Center Inside a β-Barrel Protein. *J. Am. Chem. Soc. 134*, 4216−4228.
(40) Auerbach, H., Faus, I., Wolny, J. A., Walker, F. A., Chumakov, H., Ogata, H., Knipp, M., and Schünemann, V. (2014) Nitric Oxide Heme Interactions in Nitrophorin 7 Investigated by Nuclear Inelastic Scattering. *Hyperfine Interact. 226*, 439−443.
(41) Weichsel, A., Andersen, J. F., Champagne, D. E., Walker, F. A., and Montfort, W. R. (1998) Crystal Structures of a Nitric Oxide Transport Protein from a Blood-Sucking Insect. *Nat. Struct. Biol. 5*, 304−309.
(42) Andersen, J. F., and Montfort, W. R. (2000) The Crystal Structure of Nitrophorin 2. A Trifunctional Antihemostatic Protein from the Saliva of *Rhodnius prolixus*. *J. Biol. Chem. 275*, 30496−30503.
(43) Weichsel, A., Berry, R. E., Zhang, H., Walker, F. A. and Montfort, W. R. NP2 crystal structures. PDB entries 1PEE, 1PM1, 1T68, 2A3F, 2ACP, 2AH7, 2AL0, 2ALL, 2AMM, 2ASN, 2EU7, 2HYS, and 2GTF.
(44) Andersen, J. F., Weichsel, A., Balfour, C. A., Champagne, D. E., and Montfort, W. R. (1998) The Crystal Structure of Nitrophorin 4 at 1.5 Å Resolution: Transport of Nitric Oxide by a Lipocalin-Based Heme Protein. *Structure 6*, 1315−1327.
(45) Weichsel, A., Andersen, J. F., Roberts, S. A., and Montfort, W. R. (2000) Nitric Oxide Binding to Nitrophorin 4 Induces Complete Distal Pocket Burial. *Nat. Struct. Biol. 7*, 551−554.
(46) Roberts, S. A., Weichsel, A., Qiu, Y., Shelnutt, J. A., Walker, F. A., and Montfort, W. R. (2001) Ligand-Induced Heme Ruffling and Bent NO Geometry in Ultra-High-Resolution Structures of Nitrophorin 4. *Biochemistry 40*, 11327−11337.
(47) Maes, E. M., Weichsel, A., Andersen, J. F., Shepley, D., and Montfort, W. R. (2004) Role of Binding Site Loops in Controlling Nitric Oxide Release: Structure and Kinetics of Mutant Forms of Nitrophorin 4. *Biochemistry 43*, 6679−6690.
(48) Kondrashov, D. A., Roberts, S. A., Weichsel, A., and Montfort, W. R. (2004) Protein Functional Cycle Reviewed at Atomic Resolution: Conformational Change and Mobility in Nitrophorin 4 as a Function of pH and NO Binding. *Biochemistry 43*, 13637−13647.
(49) Maes, E. M., Roberts, S. A., Weichsel, A., and Montfort, W. R. (2005) Ultrahigh Resolution Structures of Nitrophorin 4: Heme Distortion in Ferrous CO and NO Complexes. *Biochemistry 44*, 12690−12699.
(50) Montfort, W. R., Weichsel, A., and Andersen, J. F. (2000) Nitrophorins and Related Antihemostatic Lipocalins from *Rhodnius prolixus* and Other Blood-Sucking Arthropods. *Biochim. Biophys. Acta 1482*, 110−118.
(51) Orengo, C. A., Michie, A. D., Jones, S., Jones, D. T., Swindells, M. B., and Thornton, J. M. (1997) CATH: A hierarchic classification of protein domain structures. *Structure 5*, 1093−1108.
(52) Smith, L. J., Kahraman, A., and Thornton, J. M. (2010) Heme proteins: Diversity in structural characteristics, function, and folding. *Proteins 78*, 2349−2368.
(53) Ambrus, A., Friedrich, K., and Somogyi, A. (2006) Oligomerization of Nitrophorins. *Anal. Biochem. 352*, 286−295.
(54) Schanda, P., Kupce, E., and Brutscher, B. (2005) SOFAST-HMQC Experiments for Recording Two-Dimensional Heteronuclear Correlation Spectra of Proteins within a Few Seconds. *J. Biomol. NMR 33*, 199−211.
(55) Gasteiger, E., Hoogland, C., Gattiker, A., Duvaud, S., Wilkins, M. R., Appel, R. D., and Bairoch, A. (2005) Protein Identification and Analysis Tools on the ExPASy Server. In *The Proteomics Protocols Handbook* (Walker, J. M., Ed.) pp 571−607, Humana Press, Totowa, NJ.
(56) Amoia A. M. (2006) Barrel Rigidity, Heme Distortion, Ligand Protection and Nitric Oxide Interactions with Heme in Nitrophorin 4. Ph.D. Dissertation, The University of Arizona, Tucson, AZ.
(57) Murshudov, G. N., Skubak, P., Lebedev, A. A., Pannu, N. S., Steiner, R. A., Nicholls, R. A., Winn, M. D., Long, F., and Vagin, A. A. (2011) REFMACS for the refinement of macromolecular crystal structures. *Acta Crystallogr. D67*, 355−367.
(58) Potterton, E., Briggs, P., Turkenburg, M., and Dodson, E. (2003) A graphical user interface to the CCP4 program suite. *Acta Crystallogr. D59*, 1131−1137.
(59) Emsley, P., and Cowtan, K. (2004) COOT: Model-building tools for molecular graphics. *Acta Crystallogr. D60*, 2126−2132.
(60) Krissinel, E., and Henrick, K. (2004) Secondary-structure matching (SSM), a new tool for fast protein structure alignment in three dimensions. *Acta Crystallogr. D60*, 2256−2268.
(61) Amoia, A. M., and Montfort, W. R. (2007) Apo-Nitrophorin 4 at Atomic Resolution. *Protein Sci. 16*, 2076−2081.

DOI: 10.1021/bi5013047
Biochemistry 2015, 54, 208−220